Environmental Research 216 (2023) 114834

Contents lists available at ScienceDirect

Environmental Research

journal homepage: www.elsevier.com/locate/envres

Adsorption of perfluoroalkyl substances on polyamide microplastics: Effect of sorbent and influence of environmental factors

Carmen Mejías, Julia Martín, Juan Luis Santos, Irene Aparicio, Esteban Alonso *

Departamento de Química Analítica, Escuela Politécnica Superior, Universidad de Sevilla, E-41011, Seville, Spain

ARTICLE INFO

Keywords:
Microplastics
Polyamide
Emerging pollutants
Interactions
Real water samples
Vector transport

ABSTRACT

Microplastics (MPs) and perfluoroalkyl substances (PFASs) are two types of pollutants coexisting in the environment. Their co-exposure is a source of increasing concern. MPs present in the natural environment suppose an ideal surface for the sorption of hazardous contaminants. This study investigates the adsorption behaviour of six PFASs on polyamide (PA) MPs. Adsorption experiments under various internal (PA and PFASs dosage, PA particle size) and environmental (pH, ionic strength, dissolved organic matter) factors were carried out. Isotherm results (from 0.1 to 25 mg/L of PFASs) showed that the maximum adsorption capacity of the selected PFASs on the PA was as follows: perfluorooctanesulfonic acid (PFOS, 0.873 mg/g) > perfluorooctanoic acid (0.235 mg/g) > perfluoroheptanoic acid (0.231 mg/g) > perfluorohexanoic acid (0.201 mg/g) > perfluoropentanoic acid (0.192 mg/g) > perfluorobutanoic acid (0.188 mg/g) (pH 5.88, 0% salinity and 0% of dissolved organic matter). The PFOS has more tendency to be sorbed onto PA than perfluorocarboxilic acids. The MP characterization by scanning electron microscopy, X ray diffraction and Fourier transform infrared spectroscopy showed changes in the PA surface after adsorption assays. Pore filling, hydrophobic interactions and hydrogen bonds governed sorption process. The sorption capacity of PFASs was crucially affected by the PA size (from 19.6% to 99.9% for 3 mm and 50 μm particle size, respectively). The process was not significantly influenced by salinity while the dissolved organic matter exerted a negative effect (decrease from 100% to 26% for PFOS in presence of 25 mg/L of humic acid). Finally, adsorption rates of PFASs were quantified in real water matrices (influent and effluent wastewater, surface and tap water samples). The results revealed interactions between PA and PFASs and evidenced the role of PA as a vector to transport PFASs in the aquatic environment.

1. Introduction

Microplastics (MPs) are seen as important water pollutants with significant potential for health effects on organisms (Ahmed et al., 2021), which include plastic particles, films, or fibers with diameters smaller than 5 mm. Due to the slow natural degradation of MPs, and the scant removal efficiency of wastewater treatments, they can be accumulated in the environment and persist for long periods of time interacting with organisms and chemicals (Hartmann et al., 2017). Many recent investigations have been conducted on MP-related issues including their source, fate and biotoxicity in the environment (Fu et al., 2021).

The small particle size and large specific surface area of MPs make them susceptible to be vectors for adsorbing and coexisting with emerging micropollutants. Examining the adsorption behaviour of this combination is crucial for understanding the environmental concern and related problems since they may alter environmental fate, bioavailability, and biomagnification of pollutants (Duis and Coors, 2016). Perfluoroalkyl substances (PFASs) are emerging pollutants of particular concern (Martín et al., 2019). Due to their unique properties (high thermal and chemical stability), these compounds are commonly used in the production of various types of everyday products. These contaminants are ubiquitously found in industrial, urban and remote areas (Dasu et al., 2022; Kurwadkar et al., 2022). Perfluorooctanesulfonic acid (PFOS) and perfluorooctanoic acid (PFOA) are two PFASs most extensively used whereas perfluorobutanoic (PFBuA), perfluoropentanoic (PFPeA), perfluorohexanoic (PFHxA) and perfluoroheptanoic (PFHpA) acids have been frequently found in many environmental water samples (Kurwadkar et al., 2022; Dauchy et al., 2017; 2012; Martín et al., 2014). Concentrations up to 280 ng/mL and to 28 ng/L have been reported in wastewater and surface water samples, respectively (Dauchy et al., 2017; 2012). Selected compounds have been related to different

* Corresponding author. Departamento de Química Analítica, Escuela Politécnica Superior, Universidad de Sevilla, c/ Virgen de África, 7 41011, Seville, Spain.
E-mail address: ealonso@us.es (E. Alonso).

https://doi.org/10.1016/j.envres.2022.114834
Received 13 July 2022; Received in revised form 20 October 2022; Accepted 14 November 2022
Available online 15 November 2022

toxicological effects and have been reported to alter the endocrine system of organisms (Fenton et al., 2021). According to Martín et al. (2014), PFASs of short chain (PFBuA, PFPeA and PFHxA) are less frequently detected in water samples than those of longer chain but, when detected, they are present at higher concentrations. Furthermore, because of the environmental concern of PFOS and PFOA, the 3M Company voluntarily phased out their production in 2000, and replaced them by shorter-chain chemicals (Ahrens and Bundschuh, 2014; Renner, 2006).

Exposure to PFASs causes negative effects in the respiratory, reproductive, immunological, and endocrine systems (López-Arellano et al., 2019; Ballesteros et al., 2017; Keil et al., 2008). Very recently, Álvarez-Ruiz et al. (2021) assessed the bioaccumulation of four pharmaceuticals, four pesticides and four PFASs in *Mytilus galloprovincialis*. They showed that polyethylene (PE) MPs acted as a vector for the bioaccumulation of PFASs. Furthermore, they also found that removal of some PFASs was slower in the mussels exposed to MPs. In another study, Sobhani et al. (2021) estimated an increase of the bioaccumulation factor of PFOA and PFOS above 200% in earthworms exposed to polyvinylchloride (PVC)-contaminated soil. Co-exposure to MP-PFASs increased the uptake of PFOS and PFOA in earthworms and a significant decline in their reproduction.

The main factors affecting the sorption of emerging pollutants onto MPs can be divided into three categories: 1) MP type such as polarity, crystallinity, size and age; 2) Physical-chemical properties of the pollutants (pKa and Kow); 3) Environmental conditions such as salinity, temperature, pH, and dissolved organic matter. From the available literature, PE and polystyrene (PS) followed by polypropylene (PP) and PVC MPs are the preferred polymer choice for tests. Adsorption on MPs was carried out in most of the studies by considering hydrophobic and electrostatic interactions. However, PFASs present hydrophilic and polar groups in their structure, which indicates that other factors, in addition to hydrophobic interactions, such as pore filling, hydrogen and π-π bond interactions could be involved. Due to specific polymer–pollutants specific interaction, besides the influence of weathering and environmental factors, there is no rule to predict the sorption mechanism. For example, it has been reported that the sorption of antibiotics, such as sulfamethoxazole (Guo et al., 2019), and bisphenol A (Liu et al., 2019) to PS, PE, PP, PVC, and polyethylene terephthalate (PET), is lower than sorption to polyamide (PA). This fact can be related to the PA porous structure and complex hydrogen bonds (Elgarahy et al., 2021). Nylon or PA is an essential thermoplastic with amide linkage in the polymer backbone widely employed in the automotive trade, manufacture of textiles, and wind turbine (Mofakhami et al., 2020) and as consequence one of the most common polymers detected in wastewater treatments plants.

The main objective of this paper was to investigate the role of PA MPs as vector of PFASs. The study has been focused on five perfluoroalkyl carboxylic acids (PFBuA, PFPeA, PFHxA, PFHpA and PFOA) and PFOS. Common isotherm adsorption models have been applied to determine the mechanisms of MP sorption. In addition, to predict the potential influence of environmental factors on the adsorption process of MPs, parameters such as salinity, pH, and the presence of dissolved organic matter have also been evaluated. All of the analytical processes were globally considered to obtain a final conclusion. Finally, adsorption capacity of PA was also tested in four different aquatic matrices: influent and effluent wastewater, surface water and tap water.

2. Materials and methods

2.1. Chemicals and reagents

High purity standards (>99%) of PFBuA, PFPeA, PFHxA, PFHpA, PFOA and PFOS were supplied from Sigma-Aldrich (Steinheim, Germany). The structures, pKa and log K_{ow} values of PFASs are listed in Table S1, in Supplementary Material.

Table 1
Surface area and pore measurements of PA particles.

	PA particles 50 μm	PA particles 55 μm
BET surface area (m^2/g)	0.4641	0.4141
Single point surface area (m^2/g)	0.1447	0.1286
Single point desorption total pore volume (cm^3/g)	0.002995	0.001442
Desorption average pore width (nm)	19.13785	14.48313
BJH adsorption average pore diameter (4 V/A) (nm)	37.4716	28.1275

The reagents were all of high analytical grade and purity. Ammonium acetate and humic acid were supplied by Sigma-Aldrich (Madrid, Spain). Hydrochloric acid, sodium hydroxide and sodium chloride were provided by Panreac (Barcelona, Spain). Water for analysis was provided by Panreac (Barcelona, Spain). LC-MS-grade water and methanol were supplied by Biosolve BV (Valkenswaard, the Netherlands).

The different presentations of PA (powder 50 μm particle size, powder 55 μm particle size, and pellet 3 mm particle size) were provided by Goodfellow (Hamburg, Germany). The Brunauer–Emmett–Teller (BET) surface area and average adsorption and desorption pore of 50 μm PA particles were slightly higher than those of 55 μm PA particles (Table 1). Individual standards solutions at 1000 mg/L were prepared in methanol. Solutions needed in all experiments were made by dilution of this previous solution in water. The final volume of methanol in the aqueous solution used was the same for all experiments and was below 0.1% (v/v) to minimize co-solvent effect.

2.2. Microplastics characterization

The PA MP characterization was carried out using Fourier transform infrared spectroscopy (FT-IR), scanning electron microscopy (SEM), X-ray diffraction (XRD) and adsorption–desorption isotherms and accelerated surface area and porosimetry system. The FT-IR analysis was conducted with a Cary 630 FT-IR (Agilent, USA) with attenuated total reflection (ATR). Solid sample of PA does not require any preparation due to ATR technique. The spectral range was between 4000 and 400 cm^{-1} and the spectral resolution was 4 cm^{-1}. Furthermore, SEM analyses were done using a FEI-TENEO scanning electron microscope (FEI, USA). In addition, XRD patterns were obtained by a Bruker D8 Advance A25 diffractometer (Bruker, Germany) equipped with a Cu Kα radiation source operating at 40 kV and 30 mA. Diffractograms were obtained in the 2θ range of 1–70° with a step size of 0.03° and a step time of 0.1 s. The surface areas were measured from their Kr adsorption–desorption isotherms with an accelerated surface area and porosimetry system (ASAP 2420) (Micromeritics Instrument, United Kingdom) using the BET equation. The pore-size distributions were measured from the desorption of N_2 according to the Barrett–Joyner–Halenda (BJH) method. The pH_{ZPC} (pH of zero-point charge) was obtained by adjusting the pH of 50 mL of distilled water to 2, 4, 7, 9 and 11 by adding HCl or NaOH. Then, 0.5 g of PA was added and the mixture was shacked for 48 h at 25 °C. After that, the pH was measured again using a pHmeter BASIC 20 (Crison Instruments, Barcelona, Spain).

2.3. Batch experiments

A series of batch experiments were carried out to study parameters affecting the sorption capacity including the effect of PA size and dosage, PFASs concentration level, salinity, pH, and dissolved organic matter. The experiments were carried out in glass bottles, containing 0.5 g of PA and 30 mL of a stock solution containing 0.5 mg/L of a PFASs mixture. Bottles were mechanically shacked at 350 rpm using a multistirrer magnetic device (Selecta, Multimatic 9N, Spain) under a constant temperature of 25 °C for 24 h (equilibrium time). Procedural blanks without PA were prepared under the same testing conditions to

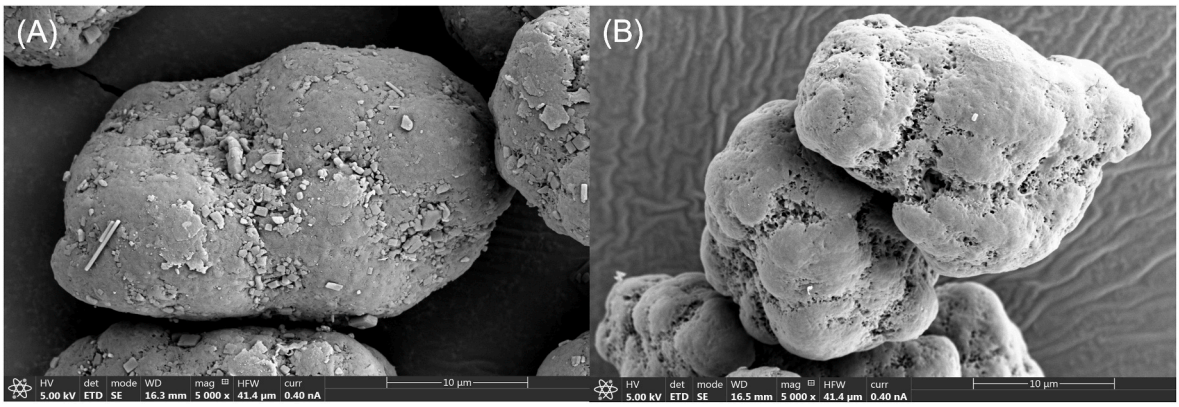

Fig. 1. SEM images of PA microplastics (A) before adsorption process, and (B) after adsorption process, magnification of 5000x.

determine the possible sorption of PFASs to the bottles or loss by volatilization. All the experiments were carried out in triplicate. Adsorption isotherms were carried out with PFASs mixture concentrations ranging from 0.1 to 25 mg/L. The PA dosage (from 0.5 to 2.4 g of PA in 30 mL of solution) and the particle size (50 µm, 55 µm and 3 mm) were also evaluated. pH values (4, 7 and 10) were adjusted by adding HCl or NaOH. The effect of salinity on adsorption was assessed adjusting NaCl concentration (from 0 to 3.5%). Pollutant solutions with humic acid concentration (from 0 to 25 mg/L) were prepared to simulate the influence of dissolved organic matter. Commonly, experiments were carried out by changing one parameter while keeping all the others at a constant level. Conditions applied in all batch experiments are summarized in Table S2.

After adsorption assay, supernatant was filtered through a 0.22 µm filter and stored until analysis. Samples were measured by direct injection into the liquid chromatography-tandem mass spectrometry (LC-MS/MS) system applying the analytical method reported by Martín et al. (2017). The chromatographic separation and MS/MS conditions are summarized in the Supplementary material (Table S3). The limits of detection and quantification were in the range from 0.3 ng/L (PFOS and PFOA) to 30 ng/L (PFBuA and PFPeA) and from 10 ng/L (PFOS and PFOA) to 100 ng/L (PFBuA and PFPeA), respectively.

2.3.1. Adsorption in environmental real conditions

Due to matrix complexity of environmental aqueous samples, adsorption studies should also include real samples. Because of that, adsorption capacity was tested in four real water samples including wastewater (influent and effluent), surface water and tap water. Wastewater samples were collected from a wastewater treatment plant located in Seville (Spain) in September 2021. Surface water samples from the Guadalquivir River (Seville, Spain) and tap water samples were collected during the same period in Seville city. The sorption experiments were carried out using 0.5 g of PA (50 µm particle size) and 30 mL of each sample matrix fortified at 0.5 mg/L of PFASs. Each matrix was characterised by pH, conductivity, chemical oxygen demand, N_T and P_T (information provided in the Supplementary Material Table S4). The quantification and correction of matrix effect was carried out by matrix-matched calibration curves.

2.4. Data analysis

The amount of adsorbed PFASs in equilibrium (q_e) was calculated as the difference between the initial concentration and concentration after the adsorption test (Eq. (1)):

$$qe=(Ci-Ce)\cdot V/m \quad (1)$$

where V (L) is the solution volume, m is the PA weight (g), Ci (mg/L) and Ce (mg/L) are the PFASs concentrations at the beginning and at the end of the adsorption experiment, respectively.

The adsorption percentage (%) was calculated according to Eq. (2):

$$\text{Adsorption } (\%)= (Ci-Ce)/Ci\cdot 100 \quad (2)$$

Linear, Langmuir and Freundlich models were used to determine the adsorbent performance to experimental isotherms (Table S5).

Correlation analysis was applied to evaluate the existence of relations between the percentage of adsorption of PFASs and the physicochemical characteristics of the water sample. Statistical analysis was carried out using Statistical 10.0 software for Windows. A correlation coefficient of 1 shows a perfect positive relationship, 0.8 shows a fairly strong positive relationship and 0.6 shows a moderate positive relationship while 0 shows a no relationship, so significant differences were considered when correlation coefficient is higher or equal tan 0.8.

3. Results and discussion

3.1. Polyamide characterization

The surface area, degree of crystallinity and morphology of MPs play a key role in the adsorption of pollutants. As it is shown in Fig. S1, PA particles are observed as pellet particles with different sizes and shapes. Approximately, the BJH adsorption average pore diameter was of 37.5 nm for 50 m µm PA MPs. These pore spaces provide extended area to micropollutants retention successfully. As can be seen in Fig. 1, PA MP particles are observed as porous material which could explain the pore filling by PFASs during the adsorption process. SEM was also used to perceive changes in surface morphology of PA MPs after the adsorption. No significant difference was observed in the size and shape of the particles (Fig. S1). Only a slightly increase in the specific surface area was observed (BET surface area from 0.46 to 0.75 m^2/g, before and after the adsorption process). XRD was used to detect crystallinity changes occurring after the adsorption and the presence of other peaks. High crystalline polymers present sharp diffraction peaks, whereas amorphous polymer diffraction peaks exhibit gentle slopes. XRD analysis of PA before adsorption is basically nylon (Fig. S2). The diffraction peaks were gentle indicating an important amorphous part. The XRD analysis after the adsorption assay with PFASs shows basically the same compounds as PA but with a higher proportion of amorphous part and with the presence of some other compounds (between 25 and 35 2θ) which could be associated with the presence of PFASs.

The ATR FT-IR spectra of PA (Fig. S3) was not much different from the spectrum previously reported (Xu et al., 2019). The obtained bands correspond to the distinctive characteristic peaks of PA MPs. The N–H stretching fits with 3300 cm^{-1} band. CH_2 symmetric and asymmetric fit with 2850 and 2950 cm^{-1} bands, respectively. Also, amides (C–N + N–H bending and C═O + C–N) fit with 1550 and 1650 cm^{-1} bands, respectively. Furthermore, amide (N–H band + C–C stretching + C═O

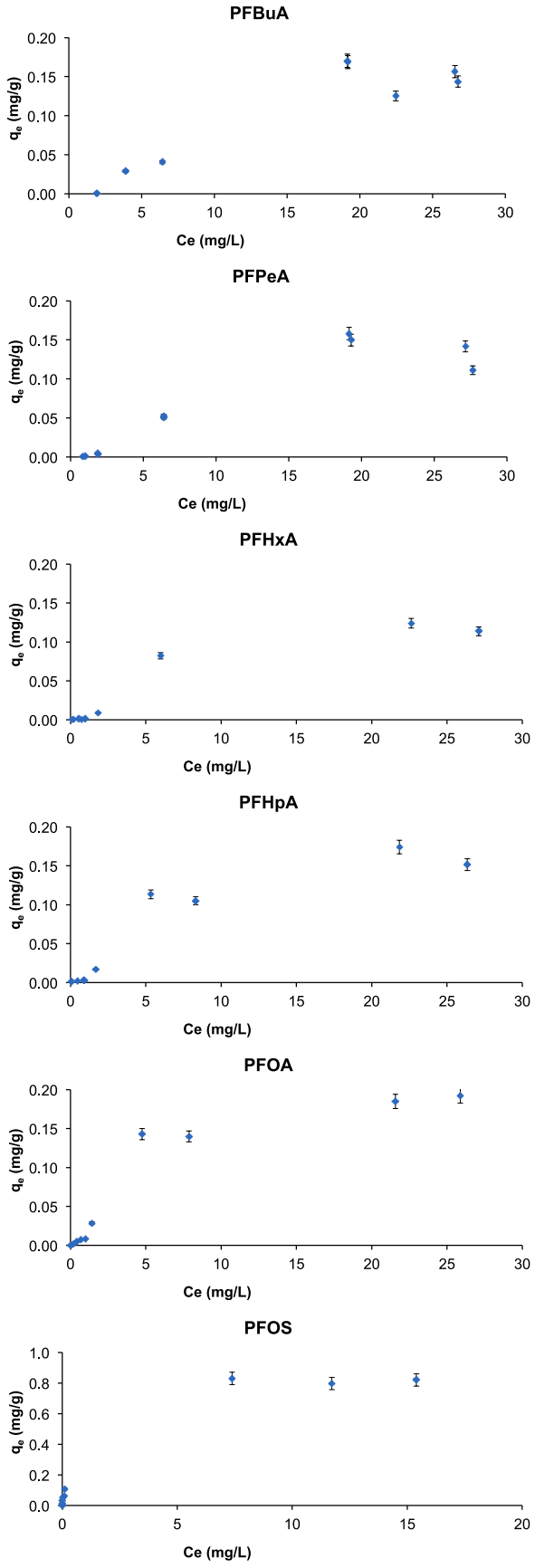

Fig. 2. Adsorption isotherms of PFASs onto PA.

bending) corresponds to 1400 cm^{-1} bands. C–N stretching is correlated with 1200 cm^{-1} bands. CCH bending (symmetric)/CH_2 twisting fit with 1000 cm^{-1} bands, and finally 800 cm^{-1} band could be associated with C–C stretching. After the PFASs adsorption test, no new peak appeared in the FTIR spectra, indicating that there was no covalent bond formed during the sorption process. Thus, the adsorption would be mainly controlled by physical interaction such as pore filling mechanism in micropores, hydrophobic interactions or the intermolecular H bonding.

3.2. Adsorption onto polyamide

Fig. 2 shows the sorption isotherms of PFASs on PA. With increasing of the PFASs concentrations, sorption sites within the PA were rapidly occupied. The sorption isotherms were generally nonlinear. Isotherm data were fitted with the Langmuir, Freundlich, and Henry models to elucidate the adsorption characteristics. The fitted parameters of the corresponding models are listed in Table S6. The Langmuir ($0.997 > R^2 > 0.845$) and Freundlich ($0.958 > R^2 > 0.776$) isotherms of PFASs fitted the data better than the Henry isotherm ($0.954 > R^2 > 0.683$). Linearity of adsorption isotherms worsen with the increase of the PFASs chain length. This fact indicates that the interactions between PFASs and PA are mono-layer adsorption processes on heterogeneous surfaces (Wang et al., 2022a). The reason for this behaviour might be in the inhomogeneous surface of PA with pores. Other parameter besides R^2 to describe the sorption behaviour is the surface heterogeneity parameter (1/n). In the Freundlich adsorption isotherm, 1/n value represents the adsorption strength between the adsorbent and the adsorbate, being weak when $0.1 < 1/n < 1.0$ (Wang et al., 2022b; Fan et al., 2021). Freundlich n values ranged from 0.387 (PFOS) to 0.547 (PFBuA). Overall, all the adsorption parameters K_L, q_{max} and K_F increase as PFASs perfluoroalkyl chain increases.

Some previous studies on the adsorption of PFOA and PFOS by PVC, PE, PS, PP, and PET are summarized in Table 2. These studies identified partitioning via hydrophobic interaction as a potential mechanism for PFAS retention onto MPs (Bhagwat et al., 2021; Ateia et al., 2020; Cormier et al., 2022; Llorca et al., 2018; Wang et al., 2015). However, unlike other hydrophobic contaminants, PFASs present besides the perfluoroalkyl chain some hydrophilic and polar groups in the head of their molecules such as COOH or SO_3H, which indicates that other factors, in addition to hydrophobic interactions, such as hydrogen bond interactions or electrostatic interactions could be involved. In a previous work, the differences in the sorption of PFOS and perfluorooctanesulfonamide (FOSA) by PE, PS, and PVC were ascribed to differences in polarity and polymer characteristics of the plastics (Wang et al., 2015). Non-ionic FOSA, which is less polar, exhibited the highest partitioning to PE, while polar PFOS exhibited the highest partitioning to PVC and the least partitioning for PS.

In this work, different adsorption capacities were observed for the selected PFASs. PFOS has a higher tendency to be sorbed onto PA than perfluorocarboxilic acids. These results agree with those from Llorca et al. (2018), which reported that this fact is an indication that the aliphatic part of the molecules is a predominant factor in their adsorption. Regarding the perfluoroalkyl carboxylic acids, the adsorption increases as their perfluoroalkyl chain increases (from 4.1% for PFBuA to 19% for PFOA and 90% for PFOS). Due to specific MPs/pollutants interaction, no rule can help predict the sorption mechanism. Since PFOA and PFOS have same chain length (C8), they should present similar hydrophobic interaction with PA particles. The different sorption capacity between PFOS and PFOA may be endorsed to their different head (sulphonic or carboxylic, respectively) functional group. For example, complex hydrogen bonding between the amide groups (proton donor) present in PA and carboxylic and sulphonic groups (proton acceptor) of PFASs structures could explain their different adsorption behaviours. Similarly, Bhagwat et al. (2021) described hydrogen bonding as other possible mechanism besides hydrophobic interactions. Authors reported that amide (−CONH−) functional groups present in

Table 2
Adsorption studies previously reported of PFASs onto various MPs.

Microplastic type	Microplastic concentration (g/L)	Particle size (μm)	Pollutant	Pollutant concentration (mg/L)	Isotherm model	Adsorption mechanism	Variables tested	Reference
PE, PS and PVC	5	150 (PE), 250 (PS) and 230 (PCV)	PFOSA and PFOS	0.005–0.05	Linear	Hydrophobic interactions	pH and presence of different ions	Wang et al. (2015)
HDPE, PS, PS-COOH and PMMA	0.005 (HDPE) and 0.002 (PS, PS-COOH, PMMA)	3-16 (HDPE), 10 (PS, PS-COOH) and 250–500 (PMMA)	PFPeA, PFBuA, PFHxA, PFHpA, PFOA, PFOS, PFNA, PFDA, PFUnA, PFDoA, PFTrA, PFTeA, PFHxDA, PFODA, PFBS, PFHxS, PFDS and PFOSA	0.001–0.02	Freundlich	Hydrophobic interactions (HDPE, PS, PS-COOH and PMMA) and van der Waals forces (HDPE)	Water sources	Llorca et al. (2018)
PE	0.05	4-6, 11–13, 20–25 and 125-500	PFOS	0.01–600	Linear	Hydrophobic interactions	Particle size	Cormier et al. (2022)
PE, PMMA, PP, PET, PS and ABS	–	75-90, (PE), 27-45 (PMMA) and <500 (PP, PET, PS, ABS)	Atrazine, PFOA, PFOS, 4-acetamidophenol and hexafluoropropylene oxide	–	–	Hydrophobic interactions	Organic matter presence	Ateia et al. (2020)
PE, PP, PES and PA	5	2000–3000	PFOS and Pb	0.005–0.05	Freundlich and linear	Hydrophobic interactions and hydrogen bonding. Presence of polarized N–H bonds.	–	Bhagwat et al. (2021)

ABS: acrylonitrile butadiene styrene; HDPE: high-density polyethylene; PA: polyamide; PE: polyethylene; PES: polyester; PET: polytethylene terephthalate; PFBS: perfluorobutanesulfonate; PFBuA: perfluorobutanoic acid; PFDA: perfluorodecanoic; PFDoA: perfluorododecanoic; PFDS: perfluorodecanesulfonate; PFHpA: perfluoroheptanoic acid; PFHxA: perfluorohexanoic acid; PFHxDA: perfluorohexadecanoic; PFHxS: perfluorohexasulfonate; PFNA: perfluorononanoic; PFOA: perfluorooctanoic acid; PFODA: perfluorooctadecanoic; PFOS: perfluorooctanesulfonic acid; PFOSA: perfluoroctanesulfonamide; PFPeA: perfluoropentanoic acid; PFTeA: perfluorotetradecanoic; PFTrA: perfluorotridecanoic; PFUnA: perfluoroundecanoic acid; PMMA: polymethyl methacrylate; PP: polypropylene; PS: polystyrene; PS-COOH: polystyrene carboxylate; PVC: polyvinyl chloride.

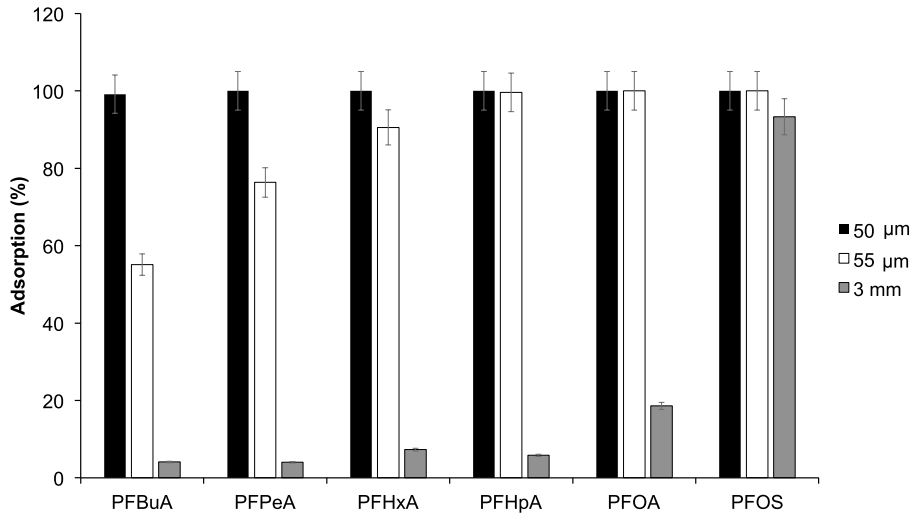

Fig. 3. Adsorption percentage (%) of PFASs onto PA with different particle size.

polyester provides sites for hydrogen bonding to ionic and polar groups of PFASs. On the other hand, besides described interactions, the high sorption capacity of PA for PFASs could be also related to its porous structure. As can be seen from SEM images, PA MPs present a high number of pores, which are mostly covered after adsorption tests.

3.3. Polyamide dosage and size

The effect of PA dosages (from 10 to 80 g/L) on the adsorption of PFASs is shown in Fig. S4. Higher MPs dosage significantly increases adsorption percentage as consequence of more available adsorption sites (t_{cal} from 4.55 (PFOS) to 19.2 (PFBuA), $t_{tab} = 1.81$; $p < 0.05$). The MP dosage equilibrium, for the amount of PFASs used in the adsorption test (500 ng/mL), was reached at 60 g/L of PA although these amounts (MP dosage and PFASs concentration) are similar or slightly higher than those found in real samples (Ragoobur et al., 2021; Wang et al., 2018; Dauchy et al., 2017).

Another factor that influences the sorption capacity is polymer size. In this regard, nanoplastics (NPs) have been found to exchange pollutants at higher rates than MPs, which seems to be related to their higher surface areas and direct proximity to polymers (Arienzo et al., 2021). In this work, a wide range (from 50 μm to 3 mm) of PA MPs size were selected among those sizes frequently found in the environment (Zhang et al., 2022; Li et al., 2021; Huang et al., 2021). The results showed that PA particles of small size (<50 μm) showed adsorption capacity higher than that of PA particles of larger size (<3 mm), which is related to their

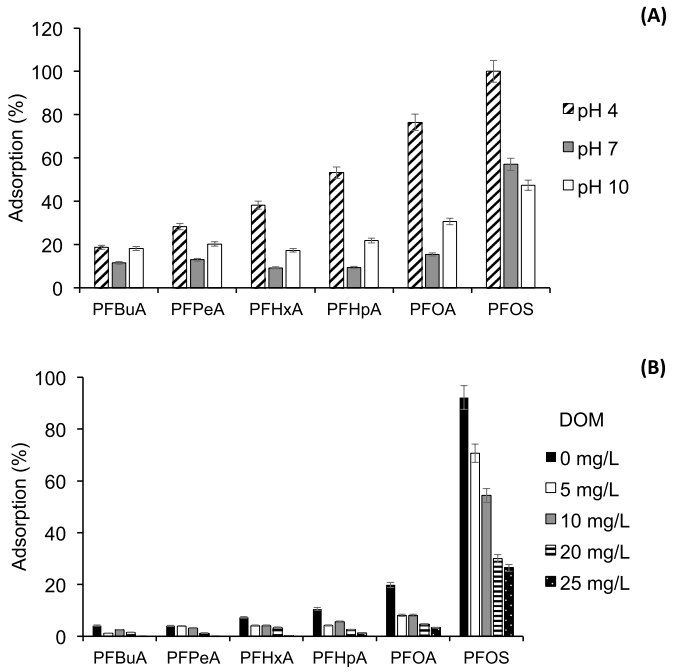

Fig. 4. Effect of pH (A) and dissolved organic matter (humic acid, mg/L) (B) on the adsorption (%) of PFASs onto PA.

higher surface area. In Fig. 3, it could be observed that the particle size of PA significantly affected the sorption of perfluoroalkyl carboxylic acids (from 99% (PFBuA) to 100% (PFOA) at 50 μm, from 55% (PFBuA) to 100% (PFOA) at 55 μm, and from 2% (PFBuA) to 18% (PFOA) at 3 mm). This fact highlights that the contact surface between sorbent and the liquid phase plays an important role in the sorption phenomena. Similar results were previously reported for PFOS with PE by Cormier et al. (2022) and for other emerging pollutants, such as the brominated flame retardants tri-n-butyl phosphate and tris(2-chloroethyl) phosphate, on PE and PVC MPs in seawater (Chen et al., 2019) or anti-inflammatory drugs on PE, PS and PP (Elizalde-Velázquez et al., 2020).

3.4. Effects of environmental factors

Environmental water matrices have a wide pH range and contain high contents of complex inorganic and organic matter. Therefore, improving our knowledge about the effect of environmental factors (pH, salinity content, dissolved organic matter) is crucial to understand adsorption potential of MPs in real water samples.

pH: Solution pH can have a significant impact on sorption since it affects both the dissociated forms of pollutants and the surface charge of the MP. Because the pK_a value of PFASs is < 3, PFASs mainly exist in anionic forms at the pH range tested (4–10). On the other hand, the pH_{PZC} (the point of zero charge) corresponds to the pH value at which the surface of the MP presents a net zero charge (Li et al., 2019). At pH < pH_{PZC}, the plastic surface will be positively charged; while at pH > pH_{PZC} the plastic surface will be negatively charged (Elizalde-Velázquez et al., 2020). The PA has a pH_{PZC} value of 6.0 (Fig. S5) and as Fig. 4A shows, acidic medium increases sorption capacity of PFASs. When pH decreased from 7 to 4, the sorption level of PFAS on PA increased from 11% to 19% for PFBuA and from 57% to 99% for PFOS. At pH > pH_{PZC}, the PA surface has a net negative charge and repulsions can be taken place which could explaine the lower adsorption at higher pH values.

Salinity effect: In this study, and particularly for PFOS, the presence of salts significantly decreases the adsorption onto PA (from 93% to 29%) whereas no significant difference was observed for the other compounds by NaCl content (Fig. S6). Llorca et al. (2018) observed a decrease of adsorption of 18 PFASs onto PE and PS in seawater in relation to freshwater that explained to be due to salinity effect. Similarly, Elizelda-Velazquez also observed that the sorption of nonsteroidal anti-inflammatory drugs onto MPs in synthetic seawater slightly decreased compared to sorption in freshwater. However, contradictory results have been reported in the literature regarding the effect of salinity. While some studies have described that salinity has a negligible effect on the sorption, others have reported that salinity increases sorption of organic compounds (Hu et al., 2020) enhancing their water solubility and increasing MP aggregation.

Dissolved organic matter: In general, a high content of dissolved organic matter decrease sorption onto MPs through its competition with pollutants to bind to sorption sites and through complexation with the hydrophobic parts of humic and fulvic acids, which modifies the partitioning between the solid surface and water (Chen et al., 2019). As can be seen in Fig. 4B, a higher concentration of humic acid (25 mg/L) results in a decrease in the adsorption percentage of PFASs onto PA (from 92% to 26%, and from 20% to 3.2%, for PFOS and PFOA, respectively), indicating a negative effect. However, the effect of dissolved organic matter was less significant for short chain PFAS (PFBuA and PFPeA).

3.5. Adsorption experiments in real water samples

Since the significant effects of dissolved organic matter and MP size on the adsorption capacity, the adsorption studies were also applied

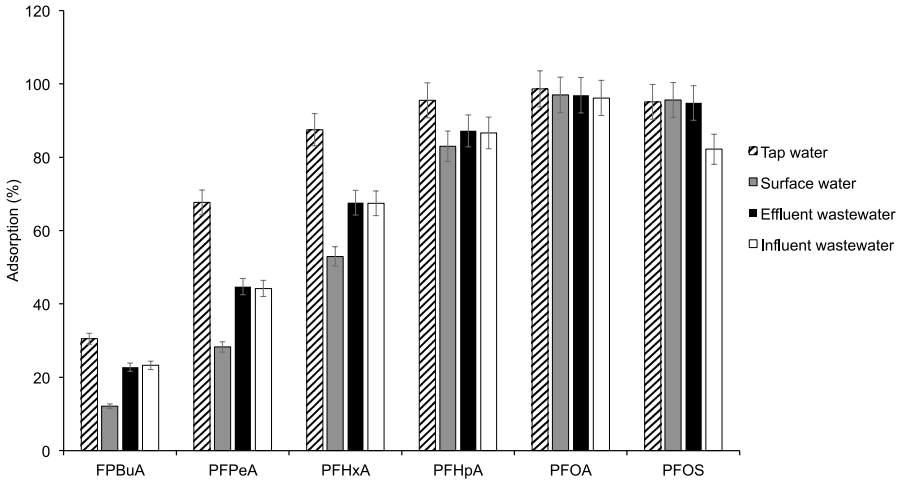

Fig. 5. Adsorption percentage (%) of PFASs onto PA in real environmental aquatic samples.

using tap water, surface water and wastewater samples to investigate the effects in real water and wastewater matrices. Experiments were carried out using fortified (0.5 mg/L) samples. Spiked concentration level was similar or slightly higher than those found in real samples (Kurwadkar et al., 2022; Podder et al., 2021; Dauchy et al., 2012, 2017). For example, concentrations up to 280 ng/mL (Dauchy et al., 2017) and up to 28 ng/mL (Dauchy et al., 2012) have been quantified in industrial wastewater treatment plants and European surface water, respectively.

In spite that these experiments are important to assess the performance of MPs in real conditions, they are not carried out in most of the adsorption studies. Concentration of PFASs are reduced considerably by PA in water samples analysed (from 12 to 31% for PFBuA to 83–100% for PFHpA, PFOA and PFOS. However, as can be seen in Fig. 5, the sorption capacities of PFASs decreased compared with the distilled water system and the influence differs for different water matrices, mainly for PFASs of short-chain (PFBuA, PFPeA and PFHxA). Correlation analysis was done considering the different environmental water matrices as cases and the physicochemical characteristics of the water and the percentage of PFASs adsorption as variables. The correlation matrix is shown in Table S7. Among all parameters, a high negative correlation was found between the conductivity and the adsorption of selected compounds (higher than −0.84). This fact could explain the slightly lowest adsorption capacity observed in surface water samples in comparison to the rest of matrices. These results demonstrated that PA may serve as a vector of PFASs in the aquatic environment with a behaviour that may differ between water matrices. Just a few studies have reported the real adsorption behaviour of micropollutants onto MPs in real aqueous samples. As an example, Arvaniti et al. (2022) studied the sorption of the pharmaceuticals valsartan and losartan onto PS MPs in bottled water, wastewater and river water, observing a decreasing of adsorption capacity in river water and wastewater compared to in bottled water.

4. Conclusions

This study investigates the interaction between widely used PFASs and PA MPs. The sorption capacity of the selected PFASs on the PA was as follows: PFOS > PFOA > PFHpA > PFHxA > PFPeA > PFBuA. The adsorption capacity increases as perfluoroalkyl chain of PFASs increases. Sorption isotherms were better fitted by non-linear models. Pore-filling, hydrophobic interactions with alkyl chains and hydrogen bonds between the amide groups in PA and sulfonic and carboxylic groups of PFASs governed the sorption process. Significantly enhanced adsorption capacity was observed for <50 μm particle size MPs PA compared to the <3 mm. The study of environmental factors affecting the PA adsorption indicated that dissolved organic matter has an adverse effect on PFAS retention. This study also provides results about real behaviour of PFASs adsorption in wastewater, surface water and tap water, resulting in a high adsorption of these compounds onto PA. Our results also reveal that PA MPs can act as vector for PFASs in real water samples and, inherently, could influence their fate. The role of MPs deserves more attention since MP could facilitate PFASs accumulation into organisms increasing their potentials risks.

Credit author statement

Carmen Mejías: Investigation, Visualization. **Julia Martín:** Conceptualization, Methodology, Writing – Original Draft. **Juan Luis Santos:** Methodology, Validation, Formal analysis. **Irene Aparicio:** Resources, Validation, Writing - Review & Editing. **Esteban Alonso:** Conceptualization, Supervision, Project administration, Funding acquisition.

Declaration of competing interest

The authors declare that they have no known competing financial interests or personal relationships that could have appeared to influence the work reported in this paper.

Data availability

Data will be made available on request.

Acknowledgements

This work was financially supported by Consejería de Economía y Conocimiento (Junta de Andalucía, Spain), Project I + D + i PAIDI Andalucía No. P20_00556. The authors wish to express their gratitude to Centro de Investigación, Tecnología e Innovación (CITIUS) at the University of Seville for PA characterization studies (with exception of FT-IR analysis). C Mejías acknowledges University of Seville for her predoctoral fellowship (VI PPIT-US 2021 II.2A).

Appendix A. Supplementary data

Supplementary data to this article can be found online at https://doi.org/10.1016/j.envres.2022.114834.

References

Ahmed, M.B., Rahman, M.S., Alom, J., Hasan, M.D.S., Johir, M.A.H., Mondal, M.I.H., Lee, D.Y., Zhou, J.L., Yoon, M.H., 2021. Microplastic particles in the aquatic environment: a systematic review. Sci. Total Environ. 775, 145793 https://doi.org/10.1016/j.scitotenv.2021.145793.

Ahrens, L., Bundschuh, M., 2014. Fate and effects of poly- and perfluoroalkyl substances in the aquatic environment: a review. Environ. Toxicol. Chem. 33 (9), 1921–1929. https://doi.org/10.1002/etc.2663.

Álvarez-Ruiz, R., Picó, Y., Campo, J., 2021. Bioaccumulation of emerging contaminants in mussel (Mytilus galloprovincialis): influence of microplastics. Sci. Total Environ. 796, 149006 https://doi.org/10.1016/j.scitotenv.2021.149006.

Arienzo, M., Ferrara, L., Trifuoggi, M., 2021. The dual role of microplastics in marine environment: sink and vectors of pollutants. J. Mar. Sci. Eng. 9 (6), 642. https://doi.org/10.3390/jmse9060642, 2021.

Arvaniti, O.S., Antonopoulou, G., Gatidou, G., Frontistis, Z., Mantzavinos, D., Stasinakis, A.S., 2022. Sorption of two common antihypertensive drugs onto polystyrene microplastics in water matrices. Sci. Total Environ. 837, 155786 https://doi.org/10.1016/j.scitotenv.2022.155786.

Ateia, M., Zheng, T., Calace, S., Tharayil, N., Pilla, S., Karanfil, T., 2020. Sorption behavior of real microplastics (MPs): insights for organic micropollutants adsorption on a large set of well-characterized MPs. Sci. Total Environ. 720, 137634 https://doi.org/10.1016/j.scitotenv.2020.137634.

Ballesteros, V., Costa, O., Iñiguez, C., Fletcher, T., Ballester, F., López-Espinosa, M.J., 2017. Exposure to perfluoroalkyl substances and thyroid function in pregnant women and children: a systematic review of epidemiologic studies. Environ. Int. 99, 15–28. https://doi.org/10.1016/j.envint.2016.10.015.

Bhagwat, G., Tran, T.K.A., Lamb, D., Senathirajah, K., Grainge, I., O'Connor, W., Juhasz, A., Palanisami, T., 2021. Biofilms enhance the adsorption of toxic contaminants on plastic microfibers under environmentally relevant conditions. Environ. Sci. Technol. 55, 8877–8887. https://doi.org/10.1021/acs.est.1c02012.

Chen, S., Tan, Z., Qi, Y., Ouyang, C., 2019. Sorption of tri-n-butyl phosphate and tris(2-chloroethyl)phosphate on polyethylene and polyvinyl chloride microplastics in seawater. Mar. Pollut. Bull. 149, 110490 https://doi.org/10.1016/j.marpolbul.2019.110490.

Cormier, B., Borchet, F., Kärrman, A., Szot, M., Yeung, L.W.Y., Keiter, S.H., 2022. Sorption and desorption kinetics of PFOS to pristine microplastic. Environ. Sci. Pollut. Res. 29, 4497–4507. https://doi.org/10.1007/s11356-021-15923-x.

Dasu, K., Xia, X., Siriwardena, D., Klupinski, T.P., Seay, B., 2022. Concentration profiles of per- and polyfluoroalkyl substances in major sources to the environment. J. Environ. Manag. 301, 113879 https://doi.org/10.1016/j.jenvman.2021.113879.

Dauchy, X., Boiteux, V., Rosin, C., Munoz, J.F., 2012. Relationship between industrial discharges and contamination of raw water resources by per uorinated compounds. Part II: case study of a uorotelomer polymer manufacturing plant. Bull. Environ. Contam. Toxicol. 89 (3), 531–536. https://doi.org/10.1007/s00128-012-0705-9.

Dauchy, X., Boiteux, V., Bach, C., Colin, A., Hemard, J., Rosin, C., Munoz, J.F., 2017. Mass ows and fate of per-and poly uoroalkyl substances (PFASs) in the wastewater treatment plant of a uorochemical manufacturing facility. Sci. Total Environ. 576, 549–558. https://doi.org/10.1016/j.scitotenv.2016.10.130.

Duis, K., Coors, A., 2016. Microplastics in the aquatic and terrestrial environment: sources (with a specific focus on personal care products), fate and effects. Environ. Sci. Eur. 28, 1–25. https://doi.org/10.1186/s12302-015-0069-y.

Elgarahy, A.M., Akhdhar, A., Elwakeel, K.Z., 2021. Microplastics prevalence, interactions, and remediation in the aquatic environment: a critical review. J. Environ. Chem. Eng. 9, 106224 https://doi.org/10.1016/j.jece.2021.106224.

Elizalde-Velázquez, A., Subbiah, S., Anderson, T.A., Green, M.J., Zhao, X., Cañas-Carrell, J.E., 2020. Sorption of three common nonsteroidal anti-inflammatory drugs

(NSAIDs) to microplastics. Sci. Total Environ. 715, 136974 https://doi.org/10.1016/j.scitotenv.2020.136974.
Fan, X., Gan, R., Liu, J., Xie, Y., Xu, D., Xiang, Y., Su, J., Teng, Z., Hou, J., 2021. Adsorption and desorption behaviors of antibiotics by tire wear particles and polyethylene microplastics with or without aging processes. Sci. Total Environ. 771, 145451 https://doi.org/10.1016/j.scitotenv.2021.145451.
Fenton, Suzanne E., et al., 2021. Per- and Polyfluoroalkyl Substance Toxicity and Human Health Review: Current State of Knowledge and Strategies for Informing Future Research. Environmental Toxicology and Chemistry 40 (3), 606–630. https://doi.org/10.1002/etc.4890.
Fu, L., Li, J., Wang, G., Luan, Y., Dai, W., 2021. Adsorption behavior of organic pollutants on microplastics. Ecotoxicol. Environ. Saf. 217, 112207 https://doi.org/10.1016/j.ecoenv.2021.112207.
Guo, X., Chen, C., Wang, J., 2019. Sorption of sulfamethoxazole onto six types of microplastics. Chemosphere 228, 300–308. https://doi.org/10.1016/j.chemosphere.2019.04.155.
Hartmann, N.B., Rist, S., Bodin, J., Jensen, L.H., Schmidt, S.N., Mayer, P., Meibom, A., Baun, A., 2017. Microplastics as vectors for environmental contaminants: exploring sorption, desorption, and transfer to biota. Integrated Environ. Assess. Manag. 13 (3), 488–493. https://doi.org/10.1002/ieam.1904.
Hu, E., Shang, S., Fu, Z., Zhao, X., Nan, X., Du, Y., Chen, X., 2020. Cotransport of naphtalene with polystyrene nanoplastics (PSNP) in saturated porous media. Effects of PSNP/naphtalene ratio and ionic strenght. https://doi.org/10.1016/j.chemosphere.2019.125602.
Huang, D., Li, X., Ouyang, Z., Zhao, X., Wu, R., Zhang, C., Lin, C., Li, Y., Guo, X., 2021. The occurrence and abundance of microplastics in surface water and sediment of the West River downstream, in the south of China. Sci. Total Environ. 756, 143857 https://doi.org/10.1016/j.scitotenv.2020.143857.
Keil, D.E., Mehlmann, T., Butterworth, L., Peden-Adams, M.M., 2008. Gestational exposure to perfluorooctane sulfonate suppresses immune function in B6C3F1 mice. Toxicol. Sci. 103, 77–85. https://doi.org/10.1093/toxsci/kfn015.
Kurwadkar, S., Dane, J., Kanel, S.R., Nadagouda, M.N., Cawdrey, R.W., Ambade, B., Struckhoff, G.C., Wilkin, R., 2022. Per- and polyfluoroalkyl substances in water and wastewater: a critical reviw of their global occurrence and distribution. Sci. Total Environ. 809, 151003 https://doi.org/10.1016/j.scitotenv.2021.151003.
Li, Z., Mei, Q., Chen, L., Zhang, H., Dong, B., Dai, X., He, C., Zhou, J., 2019. Enhancement in adsorption potential of microplastics in sewage sludge for metal pollutants after the wastewater treatment process. Water Res. 157, 228–237. https://doi.org/10.1016/j.watres.2019.03.069.
Li, J., Ouyang, Z., Liu, P., Zhao, X., Wu, R., Zhang, C., Lin, C., Li, Y., Guo, X., 2021. Distribution and characteristics of microplastics in the basin of chishui river in renhuai, China. Sci. Total Environ. 773, 145591 https://doi.org/10.1016/j.scitotenv.2021.145591.
Liu, X., Shi, H., Xie, B., Dionysiou, D.D., Zhao, Y., 2019. Microplastics as both a sink and a source of bisphenol A in the marine environment. Environ. Sci. Technol. 53, 10188–10196. https://doi.org/10.1021/acs.est.9b02834.
Llorca, M., Schirinzi, G., Martínez, M., Barceló, D., Farré, M., 2018. Adsorption of perfluoroalkyl substances on microplastics under environmental conditions. Environ. Pollut. 235, 680–691. https://doi.org/10.1016/j.envpol.2017.12.075.
López-Arellano, P., López-Arellano, K., Luna, J., Flores, D., Jiménez-Salazar, J., Gavia, G., Teteltitla, M., Rodríguez, J.J., Domínguez, A., Casas, E., Bahena, I., Betancourt, M., González, C., Ducolomb, Y., Bonilla, E., 2019. Perfluorooctanoic acid disrupts gap junction intercellular communication and induces reactive oxygen species formation and apoptosis in mouse ovaries. Environ. Toxicol. 34, 92–98. https://doi.org/10.1002/tox.22661.
Martín, J., Camacho-Muñoz, D., Santos, J.L., Aparicio, I., Alonso, E., 2014. Determination of emerging and priority industrial pollutants in surface water and wastewater by liquid chromatography-negative electrospray ionization tandem mass spectrometry. Anal. Bioanal. Chem. 406, 3709–3716. https://doi.org/10.1007/s00216-014-7689-8Mofakhami.
Martín, J., Zafra-Gómez, A., Hidalgo, F., Ibáñez-Yuste, A.J., Alonso, E., Vílchez, J.L., 2017. Multi-residue analysis of 36 priority and emerging pollutants in marine echinoderms (*Holothuria tubulosa*) and marine sediments by solid-liquid extraction followed by dispersive solid phase extraction and liquid chromatography–tandem mass spectrometry analysis. Talanta 166, 336–348. https://doi.org/10.1016/j.talanta.2017.01.062.
Martín, J., Hidalgo, F., García-Corcoles, M.T., Ibáñez-Yuste, A.J., Alonso, E., Vilchez, J.L., Zafra-Gómez, A., 2019. Bioaccumulation of perfluoroalkyl substances in marine echinoderms: results of laboratory-scale experiments with *Holothuria tubulosa* Gmelin, 1791. Chemosphere 215, 261–271. https://doi.org/10.1016/j.chemosphere.2018.10.037.
Podder, A., Sadmani, A.H.M.A., Reinhart, D., Chang, N., Goel, R., 2021. Per and poly-fluoroalkyl substances (PFAS) as contaminant of emerging concern in surface water: a transboundary review of their occurrences and toxicity effects. J. Hazard Mater. 419, 126361 https://doi.org/10.1016/j.jhazmat.2021.126361.
Ragoobur, D., Huerta-Lwanga, E., Somaroo, G.D., 2021. Microplastics in agricultural soils, wastewater effluents and sewage sludge in Mauritius. Sci. Total Environ. 798, 149326 https://doi.org/10.1016/j.scitotenv.2021.149326.
Renner, R., 2006. The long and the short of perfluorinated replacements. Environ. Sci. Technol. 40 (1), 12–13. https://doi.org/10.1021/es062612a.
Sobhani, Z., Fang, C., Naidu, R., Megharaj, M., 2021. Microplastics as a vector of toxic chemicals in soil: enhanced uptake of perfluorooctane sulfonate and perfluorooctanoic acid by earthworms through sorption and reproductive toxicity. Environ. Technol. Innovat. 22, 101476 https://doi.org/10.1016/j.eti.2021.101476.
Mofakhami, E., Tencé-Girault, S., Perrin, J., Scheel, M., Gervat, L., Ovalle, C., Laiarinandrasana, L., Fayolle, B., Miquelard-Garnier, G., 2020. Microstructure-mechanical properties relationships in vibration welded glass-fiber-reinforced polyamide 66: a high-resolution X-ray microtomography study. Polym. Test. 85, 106454 https://doi.org/10.1016/j.polymertesting.2020.106454.
Wang, F., Shih, K.M., Li, X.Y., 2015. The partition behavior of perfluorooctanesulfonate (PFOS) and perfluorooctanesulfonamide (FOSA) on microplastics. Chemosphere 119, 841–847. https://doi.org/10.1016/j.chemosphere.2014.08.047.
Wang, T., Zou, X., Li, B., Yao, Y., Li, J., Hui, H., Yu, W., Wang, C., 2018. Microplastics in a wind farm area: a case study at the rudong offshore wind farm, yellow sea, China. Mar. Pollut. Bull. 128, 466–474. https://doi.org/10.1016/j.marpolbul.2018.01.050.
Wang, X., Zhang, R., Li, Z., Yan, B., 2022a. Adsorption properties and influencing factors of Cu(II) on polystyrene and polyethylene terephthalate microplastics in seawater. Sci. Total Environ. 812, 152573 https://doi.org/10.1016/j.scitotenv.2021.152573.
Wang, Y., Van Zwieten, L., Wang, H., Wang, L., Li, R., Qu, J., Zhang, Y., 2022b. Sorption of Pb(II) onto biochar is enhanced through co-sorption of dissolved organic matter. Sci. Total Environ. 825, 153686 https://doi.org/10.1016/j.scitotenv.2022.153686.
Xu, P., Ge, W., Chai, C., Zhang, Y., Jiang, T., Xia, B., 2019. Sorption of polybrominated diphenylethers by microplastics. Mar. Pollut. Bull. 145, 260–269. https://doi.org/10.1016/j.marpolbul.2019.05.050.
Zhang, Y., Peng, Y., Xu, S., Zhang, S., Zhou, G., Yang, J., Li, H., Zhang, J., 2022. Distribution characteristics of microplastics in urban rivers in Chengdu city: the influence of land-use type and population and related suggestions. Sci. Total Environ. 846, 157411 https://doi.org/10.1016/j.scitotenv.2022.157411.